

## Robust $H_\infty$ , $H_2/H_\infty$ Controller for Rotational/Translational Actuator (RTAC)

R. Adlgostar, H. Azimian and H. D. Taghirad, *Member, IEEE*,

**Abstract**— In this paper, robust controllers have been proposed for oscillation suppression in the RTAC benchmark problem. A nominal plant and an uncertainty model are extracted out of varieties of linear models, identified for the nonlinear system and the generalized plant for the unstructured uncertainty problem has been presented. Based on passivity, a cascade controller has been designed to reduce amount of uncertainty in lower frequencies. It is verified that through a nonlinear feedback controller in the inner loop, the uncertainty of linear estimates of the system reduces significantly, and becomes plausible to use linear robust techniques such as mixed sensitivity and  $H_2/H_\infty$  to design controller for the system. Finally  $H_\infty$  and  $H_2/H_\infty$  controllers have been designed for new generalized plant and results are compared with the previous reports in literature.

### I. INTRODUCTION

THE Rotational/Translational Actuator (RTAC) experiment has originally been studied as a simplified model of a dual-spin spacecraft. It has been shown that this system have similar averaged dynamic behavior to that of a dual-spin spacecraft [1]. Later, the RTAC system has been studied to investigate the use of a rotational actuator for stabilizing translational motion [2]. In this nonlinear system, unlike a linear actuator, the actuator stroke limitations are implicitly involved in the system dynamics [3]. Consider the translational oscillator with an eccentric rotational proof mass shown in Fig 1. The oscillator consists of a cart of mass  $M$  connected to a fixed wall by a linear spring of stiffness  $k$ . The motion is confined in one direction and is merely in the horizontal plane so that gravitational forces do not contribute. The proof mass attached to the cart has mass  $m$  and moment of inertia  $I$  about its center of mass, which is located at a distance  $e$  from the point about which the proof mass rotates.  $N$  denotes the control torque applied by the rotational actuator to the proof mass, and  $F$  is the disturbance force on the cart.

In this nonlinear benchmark problem, the control objective is the oscillator stabilization and external disturbances rejection despite the limited control torque provided by the rotational actuator. A number of research works are reported on this problem. For instance, Bupp, Bernstein and Coppola implement four nonlinear controllers on the RTAC, including an integrator back-stepping controller and three passivity-based controllers [4]. Also Jankovic,

Fontaine and Kokotovic design and compare linear cascade controllers and passivity-based controllers for the system [5]. Kanellakopoulos and Zhao design a back-stepping controller for tracking [6], and Jiang and Kanellakopoulos design an output feedback controller through observer/ controller back-stepping design [7]. Mracek and Cloutier use the state-dependent Riccati equation technique to produce a nonlinear controller for the benchmark problem [8]. Kolmanovsky and McClamroch propose a hybrid feedback control law expressed in terms of a continuous feedback part and a part including switched parameters [9].

As it is explained, the abovementioned research conducts nonlinear control synthesis for the system, since the RTAC exhibits coupled nonlinear dynamic equations. It is only in [10] that a linear identification of the system is proposed and linear  $H_\infty$  controller is designed for the system, and the performance limitations due to the actuator saturations are observed. In this paper a methodology to design linear controller for RTAC is developed for the disturbance rejection objective, in presence of actuator efforts limitations. To accomplish that a linear identification technique is forwarded not only for the control effort input to oscillation of the cart, but the dynamical behavior of the disturbance is also estimated. Furthermore, the deviation of nonlinear dynamics of the system is encapsulated into norm bounded multiplicative uncertainty. By this means linear robust techniques such as  $H_\infty$ ,  $H_2/H_\infty$  and  $\mu$ -synthesis are applied to the system and the closed loop performances are compared.

### II. SYSTEM MODELING

Assuming that the system operates in a horizontal plane, the equations of motions of RTAC system are reviewed in the following [9]:

$$\begin{cases} (M+m)\ddot{q} + kq = -me(\ddot{\theta} \cos \theta - \dot{\theta}^2 \sin \theta) - (b+c)\dot{q} + F, \\ (I+me^2)\ddot{\theta} = -me\dot{q} \cos \theta + N \end{cases} \quad (1)$$

In which,  $q$  denotes the translational position of the cart, and  $\theta$  denotes the angular position of the rotational proof mass as illustrated in figure 1. Using the following normalized variables, results in the normalized equations of motion.

$$\begin{aligned} \xi &= \sqrt{(M+m)/(I+me^2)} q; \quad \tau = \sqrt{k/(M+m)} t \\ v &= \sqrt{(M+m)/k(I+me^2)} N \end{aligned} \quad (2)$$

$$\begin{cases} \ddot{\xi} + \xi = \varepsilon(\dot{\theta}^2 \sin \theta - \ddot{\theta} \cos \theta) - (b+c)/\sqrt{k(M+m)} \dot{\xi} + D \\ \ddot{\theta} = -me\dot{q} \cos \theta + v \end{cases} \quad (3)$$

Where  $D$ ,  $v$ ,  $\xi$  denote the disturbance, normalized torque and normalized displacement of the cart, respectively.

Authors are with the K.N. Toosi University of Technology, Electrical Engineering Department, Advanced Robotics and Automated System (ARAS), P.O. Box 16315-1355, Tehran, IRAN. (Phone: +98-21-846-2026; E-mail: Taghirad@kntu.ac.ir, R\_Adlgostar@sina.kntu.ac.ir, H\_Azimian@sina.kntu.ac.ir)

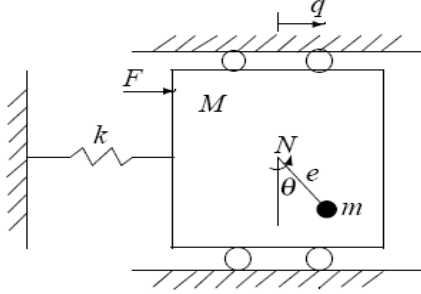


Figure 1. Control structure under model perturbations

Numerical values used for the system are as follows:

$M=1$  kg,  $m=0.1$  kg,  $k=186$  N/m,  $e=0.06$  m,  $I=2.2e^{-4}$  gcm<sup>2</sup> which, results in:  $\tau=13$  t (where,  $t$  is the time in seconds),  $\zeta=43.5494$  q,  $v=3.1932$  N, and having the normalized parameter:

$$\varepsilon = me / \sqrt{(I + me^2)(M + m)} = 0.237.$$

In all simulations used in this paper the above parameters are used and in figures, the normalized  $\tau$  is considered for the time axis. In order to obtain more insight into the dynamic behavior of the system, the nonlinear equations of motions are linearized about the equilibrium point  $(0, 0, \theta_0, 0)^T$ :

$$A = \frac{1}{1 - \varepsilon^2 \cos^2 \theta_0} \begin{bmatrix} 0 & 1 - \varepsilon^2 \cos^2 \theta_0 & 0 & 0 \\ -1 & 0 & 0 & 0 \\ 0 & 0 & 0 & 1 - \varepsilon^2 \cos^2 \theta_0 \\ \varepsilon \cos \theta_0 & 0 & 0 & 0 \end{bmatrix} \quad (4)$$

$$B_1 = \begin{bmatrix} 0 \\ -\varepsilon \cos \theta_0 / (1 - \varepsilon^2 \cos^2 \theta_0) \\ 0 \\ 1 / (1 - \varepsilon^2 \cos^2 \theta_0) \end{bmatrix}, B_2 = \begin{bmatrix} 0 \\ 1 / (1 - \varepsilon^2 \cos^2 \theta_0) \\ 0 \\ -\varepsilon \cos \theta_0 / (1 - \varepsilon^2 \cos^2 \theta_0) \end{bmatrix}$$

In which the states are:  $(\xi, \dot{\xi}, \theta, \dot{\theta})^T$  and the last two  $B_i$ 's correspond to the following input-output linear transfer functions of torque and disturbance, respectively:

$$\zeta / v = \frac{\varepsilon \cos \theta_0}{(\varepsilon^2 \cos^2 \theta_0 - 1)s^2 - 1}, \quad \zeta / D = \frac{1 - \varepsilon \cos \theta_0}{(1 - \varepsilon^2 \cos^2 \theta_0)s^2 + 1} \quad (5)$$

Analyzing these linear models, it is observed that at  $\theta=\pi/2$  the system is not controllable, and hence the system operation should be avoided close to this range. Moreover, term  $\varepsilon \cos \theta_0$  in the transfer functions produces a configuration dependent DC gain to the system. Thus, if any linear model for the system is nominated, there would be a large variation in its frequency response at low frequencies [9]. No friction is considered for the system in the above formulation. However, in practice there is always some friction to the system, which damps out the sustained oscillations. To consider the friction effect, viscous friction is added to the system dynamics, and the above transfer functions are recalculated. This transfer function has two damping poles at  $-0.0004 \pm 1.03i$  which introduces a negligibly damping response.

$$\zeta / v = \frac{\varepsilon \cos \theta_0}{(\varepsilon^2 \cos^2 \theta_0 - 1)s^2 - \frac{T_v}{\sqrt{k(M+m)}}s - 1} \quad (6)$$

### III. LINEAR IDENTIFICATION

In order to apply Linear robust controller design to this problem, the nonlinear model of RTAC is represented by a linear model and multiplicative uncertainty, using a systematic linear identification scheme. In this representation, the nominal model replicates the dynamic behavior of the system, only at nominal conditions, and all nonlinear interactions, un-modeled dynamics and the disturbances are encapsulated via an unstructured uncertainty representation. This idea is used extensively in many applications, where linear  $H_\infty$  schemes are used in controller design of some nonlinear systems [11].

In order to represent a system into this form, suppose the true system belongs to a family of plants  $\Pi$ , which is defined by using the following perturbation to the nominal plant  $P_o$ :

$$\forall P(s) \in \Pi \quad P(s) = (1 + \Delta(s)W(s))P_o(s) \quad (7)$$

In this equation  $W(s)$  is a stable transfer function indicating the upper bound of uncertainty and  $\Delta(s)$  indicates the admissible uncertainty block, which is a stable but unknown transfer function with  $\|\Delta\|_\infty < 1$ . In this general representation  $\Delta(s)W(s)$  describes the normalized perturbation of the true plant from nominal plant, and is quantitatively determined through identification at each frequency:

$$\frac{P(j\omega)}{P_o(j\omega)} - 1 = \Delta(j\omega)W(j\omega) \quad (8)$$

In which  $\|\Delta\|_\infty < 1$ ; hence,

$$\left| \frac{P(j\omega)}{P_o(j\omega)} - 1 \right| \leq |W(j\omega)|, \quad \forall \omega \quad (9)$$

Where,  $|W(j\omega)|$  represents the amplitude of the uncertainty profile with respect to frequency. Nominal plant  $P_o$ , can be evaluated experimentally, through a series of frequency response estimates of the system in the operating regime [12]. Linear identification for the system can be applied with different input amplitudes, while their outputs are measured and logged. By minimizing the least squares of the prediction error, from the set of input-output information, a set of linear models are estimated for the system, which can be considered as the set  $\Pi$ . The uncertainty upper bound  $W(s)$ , is then obtained using Equation (9), while the nominal plant  $P_o$  is selected from the average fit over all the individual identified plants. By this means, not only the nominal plant of the system is obtained, but also a measure of its perturbations, will be encapsulated by the multiplicative uncertainty. This representation is highly effective, if the system variations from its nominal conditions are not large, especially within the desired closed-loop bandwidth of the system.

In order to identify the nominal transfer function and uncertainty profile, random and chirp signals (0.1 to 10 Hz) are employed to excite all modes of the system. Inputs amplitude are chosen such that the system doesn't exceed our desired working range ( $-\pi/3 < \theta < \pi/3$  and the cart displacement is limited to 10 cm). Among different methods, the OE method gives best fitness to the system outputs, considering a fourth order nominal model. Tustin

method has been employed to obtain continuous proper models from the identified discrete time models.

Forwarding this approach with no internal feedback for the open loop system leads to an uncertainty profile whose magnitude is more than 0 dB in all frequencies. Therefore, the uncertainty profile is too large in this case to design an  $H_\infty$  controller and some internal feedback loops are used to remedy this problem. First, a linear internal feedback  $u = -k_1\theta - k_2\dot{\theta}$  proposed in [2], is employed to reduce the uncertainty. Based on the above considerations in identification, the nominated plant is derived as:

$$p_0(s) = \frac{(s+0.058)(s-0.037)(s+41.54+32.98i)(s+41.54-32.98i)}{(s+9.4)(s+2.58)(s+0.0038-0.99i)(s+0.0038+0.99i)} \quad (10)$$

The system has two oscillatory poles close to the origin and two stable poles. Also there is one unstable zero in RHP so we are alerted to dealing with a non-minimum phase system. Using equation (9) the uncertainty profile upper bound is obtained as:

$$W_i(s) = \frac{0.75(s+1/10)(s+1/50)}{(s+1/30)(s+1/1000)} \quad (11)$$

It shows that our effort is paid off in order to reduce the uncertainty profile as it is below the 0 dB in low and middle frequencies.

Although the linear cascade feedback paves the way for designing an  $H_\infty$  controller, a nonlinear cascade feedback  $u(t) = -k_1 \sin \theta - k_2 \dot{\theta}$  proposed in this paper, because of two main reasons. First, by using this kind of feedback, the equilibrium point can be changed to  $2\pi M$  (where  $M$  is an integer), by which extra windings of the arm are avoided and the control force is limited [6]. Secondly, the sinusoidal term compensates the nonlinearity of the numerator of the transfer function given in equation (6). Forwarding the same procedure as before, the identified models, the nominal plant and the disturbance model are illustrated in figure 2.

The nominal plant transfer function is:

$$p_0(s) = \frac{(s+0.03)(s-0.0297)(s+93.65)(s-100.15)}{(s+5.2-1.97i)(s+5.2+1.97i)(s+0.0037-0.99i)(s+0.0037+0.99i)} \quad (12)$$

And the upper bound of the uncertainty profile is:

$$W_i(s) = \frac{0.3528s^4 + 2.562s^3 + 4.662s^2 + 3.57s + 1.05}{0.03s^4 + 12s^3 + 900.8s^2 + 60.01s + 1} \quad (13)$$

Comparing the above transfer function with that of linear cascade feedback shows that the dominant behavior of both cases, are almost the same.

As we see in figure 2.a the system has more uncertainty in lower frequencies than that of in mid frequencies. The least uncertainty occurs in dominant frequency where the effect of other modes is diminished.

The disturbance to output transfer function also obtained here has a similar manner in dominant frequency of the system. However, the uncertainty in this case is very small and is negligible in design procedure. Obtained models are depicted in figure 2. The dominant poles of the disturbance transfer function are the same as the system dominant poles which it verifies the validity of our identification. The disturbance transfer function is:

$$p_d(s) = \frac{(s+4.5+2.6i)(s+4.5-2.6i)(s+94.6)(s-100.02)}{(s+4.7+2.3i)(s+4.7-2.3i)(s+0.0038-0.99i)(s+0.0038+0.99i)} \quad (14)$$

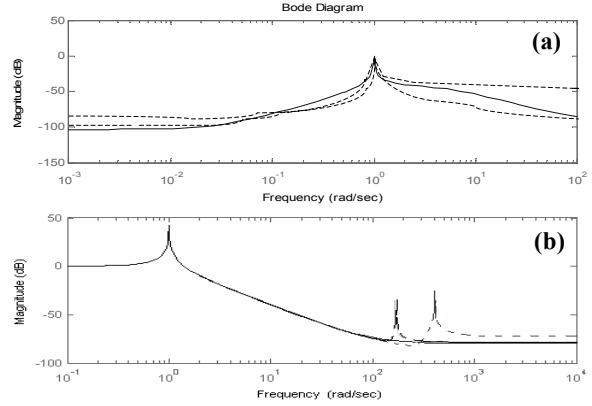


Figure 2. a) Frequency response of estimated and nominal plants b) Frequency response estimated and nominal models for disturbance

#### IV. $H_\infty$ CONTROLLER DESIGN

Since the required objectives of robust stability and disturbance attenuation despite the limited control effort, are well suited into an  $H_\infty$  design framework, in this section the RTAC general controller design is reformulated such that this methodology can be applied. The objectives of controller design are robust stability and disturbance rejection, despite the limited control effort. All these objectives can be simultaneously optimized by the solution of a mixed-sensitivity problem formulated on the generalized plant illustrated in figure 3. The robust stability is guaranteed by minimizing the infinity norm of weighted transfer function from  $d$  to  $z_1$ , which is equivalent to the weighted complementary sensitivity function:  $\|W_i T\|_\infty < I$  (Small-gain theorem). The tracking performance and disturbance attenuation is obtained by minimizing the infinity norm of  $d$  to  $z_2$ , or the weighted sensitivity function  $\|W_{perf} S\|_\infty < I$ .

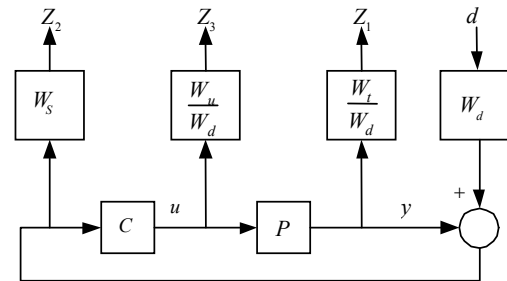


Figure 3. Block diagram representation of mixed- sensitivity solution.

Finally, the infinity norm of  $d$  to  $z_3$ , or weighted control effort transfer function penalizes controllers with high control effort, and provides a media in our optimization to include directly the control effort limitations into the controller synthesis. Hence, by simultaneously optimization of the infinity norm of the transfer matrix  $\|T_{yz}\|_\infty < I$ , all the objectives are satisfied, provided that a solution to the mixed-sensitivity problem exists. Many tractable numerical solutions exist for this problem [12]. This framework can be formulated in the following problem.

**Problem 1.** Design a controller  $C(s)$  in the feedback loop illustrated in figure 3, such that the following multi-objective suboptimal problem is solved.

$$\left\| \begin{array}{l} W_t(s)T(s) \\ W_{perf}(s)S(s) \\ W_u(s)U(s) \end{array} \right\|_{\infty} \leq 1 \quad (15)$$

This problem can be solved numerically using the `hinfsyn` function of robust toolbox of MATLAB [12]. Note that the function  $W_u(s)$  can be chosen simply to be a constant at all frequencies,  $W_u(s) = \Omega$ , which leads to  $\|U(s)\|_{\infty} < 1/\Omega$ . This selection limits the magnitude of  $U(s)$  at all frequencies, and therefore, causes limitations on the closed-loop bandwidth. As an alternative, the control effort weighting function  $W_u(s)$ , can be shaped in the frequency domain. Obviously reducing the function  $W_u(s)$  in high frequencies will result in decreasing the level of the control action fast transients (or jumps), and hence, generally decreases the total amplitude of  $u(t)$ . This fact is verified in simulation studies.

Instead of frequency shaping of the  $W_u(s)$  the two-norm of  $U(s)$  can be chosen as the subject of the optimization. Limiting the two norm or the energy of  $u(t)$  is more appropriate to the general objective of limiting the control effort in the closed-loop system. This idea will be elaborated in the next section.

#### A. Design Road Map

In the design we just deal with pulse-shape disturbances. From the physical dynamics perspective of this system, it is clear that we can never attenuate step disturbances, in the sense of continuous force acting on the cart. Therefore, in this design we are aiming to attenuate pulse-shape disturbances as rapidly as possible. As studied in the previous section, the 50db-amplitude of  $\zeta D$ - aptly named  $W_d$  - significantly amplifies the disturbance around the nominal frequency of the system (1rad/sec). It is worth remembering that the dominant poles of this transfer functions are at  $0.0037+j0.998$  and  $0.0037-j0.998$  by which we can predict an impulse response that has a slow oscillatory response with frequency of 1rad/sec where the other modes of the system may decay in a short transient. It sounds logical to compensate the effect of  $W_d$  by setting  $S_{id} = W_s^{-1} = (W_d F)^{-1}$ , where  $F$  is a shaping filter which provides some degrees of freedom, by using  $W_{perf} = W_d W_s$ . It is ideal to suppress  $W_d$  in all frequencies, However, there are satisfying reasons for the failure of extensive trials for such achievement. In fact due to the ‘‘Waterbed Effect’’ phenomenon it is impossible to design  $W_s$  for a significant attenuation of the disturbance in all frequencies. Literally ‘‘Waterbed effect’’ happens for non minimum phase systems as a result of bandwidth limitation caused by interpolation condition. Using Bode’s integrals Theorem we have:

$$\int_0^{\infty} \log |S(j\omega)| d\omega = \pi \sum p_i = 0 \quad (16)$$

Since the integral of the  $\log |S(j\omega)|$  must be zero it is obvious that a large negative peak around resonance

frequency must be compensated by a negligible positive gain in all other frequencies. On the other hand, if we could decrease sensitivity at lower frequencies we could achieve disturbance rejection objective simultaneously with step response tracking. However, consider that tracking of a step is not plausible due to the nature of the system. Restating our design policy; we are aiming to cancel two dominant slow poles of the system. Considering our nominal plant we find that we have two positive zeros: One at 0.029 rad/sec and the other at 100.15 rad/sec. According to the interpolation condition, sensitivity complementary should attain two zeros at those frequencies. In other word, the slope of magnitude of  $T$  should increase by 20dB/dec at each of these frequencies. Also consider that these RHP zeros behave like stable poles in the phase plot of  $T$ . So, although we can not attenuate disturbance at all frequencies, we should try in a way that those frequencies are not amplified either. This reasoning leads to choosing a smooth  $W_s$ , which acts as a notch filter at 1rad/sec as depicted in figure 4(b).

$$W_s = \frac{-0.174 s^6 - 1.017 s^5 + 1649 s^4 + 1.856e4 s^3 + 7.91e4 s^2 + 1.128e5 s + 4.73e4}{s^6 + 262.8 s^5 + 1.833e4 s^4 + 1.593e5 s^3 + 4.754e5 s^2 + 1.621e5 s + 4.551e5} \quad (17)$$

Next we determine appropriate  $W_u$  to impose the desired limitation on the control effort. Including this transfer function into mixed sensitivity problem may force some restrictions to the performance and may result in a more conservative design. For, we are minimizing the infinity norm of  $W_u U$  which means restricting the peak of an induced norm of the corresponding system. Since we need to have nominal performance around the oscillation frequency of the system, the key point to determine appropriate  $W_u$  is that the control torque at those frequencies must be permitted to be larger than that of in other frequencies. Such trend results in a band-stop  $W_u$  which traps signals at frequency 1rad/sec with an attenuation of 50db, as illustrated in figure 4(a)

$$W_u = \frac{0.8971 s^4 + 4.517 s^3 + 15.82 s^2 + 9.213 s + 19.33}{s^4 + 24.8 s^3 + 87.35 s^2 + 414.1 s + 21.38} \quad (18)$$

The optimal solution to this problem is achieved with  $\gamma_{opt}=0.96$  while the resulting controller is of order 18. Some convenient methods of order reduction can also be employed to obtain lower order controllers.

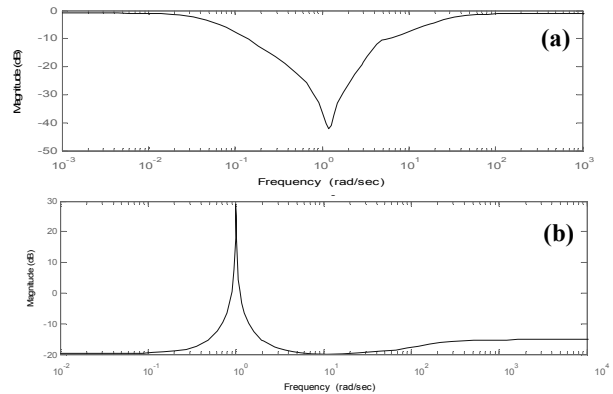


Figure 4. Bode plot of a)  $W_u$  b)  $W_s$

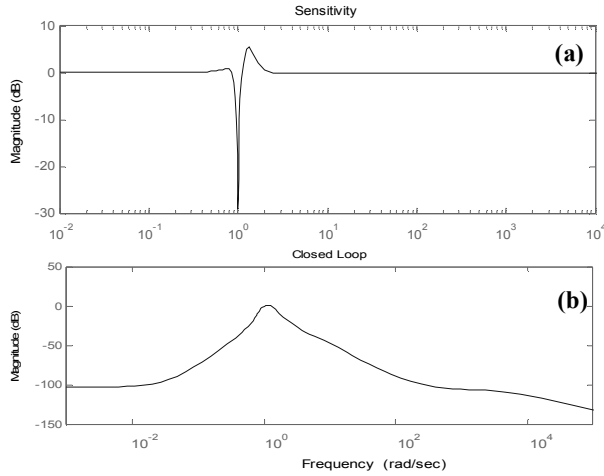


Figure 5. Bode plot of sensitivity (a) and the closed loop (b)

Also the resulting sensitivity function, as is illustrated in figure 5(a), is acceptably smooth with the desired rejection at 1rad/sec, but with a small resonant of about 5dB at 1.7rad/sec. The closed loop, depicted in figure 5(b), has a satisfactory bandwidth of about 0.5rad/sec. Also we have achieved 0dB at 1rad/sec; this means a neat Tracking and disturbance rejection at this frequency. Therefore, we have satisfied two significant control objectives (disturbance rejection and tracking) at dominant frequency of the system.

As illustrated in figure 6(a), nominal performance is attained critically with a peak at 1rad/sec. We have achieved nominal performance here but it could be more satisfactory if the nominal performance is smoother over a wide range of frequency.

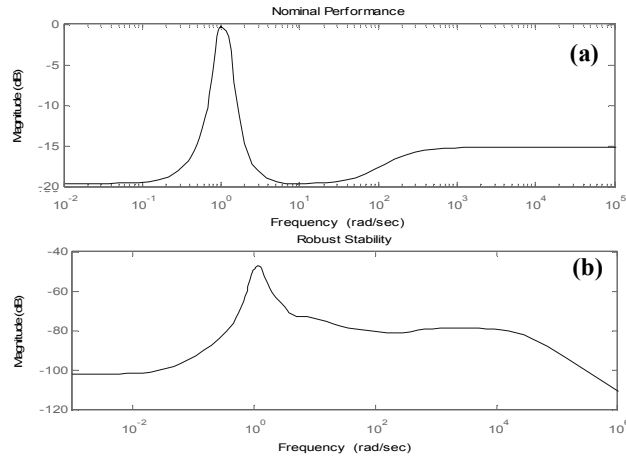


Figure 6. Nominal performance  $W_{perf}S$  (a) and Robust stability  $W_rT$  (b)

According to figure 6(b), in which the frequency response of  $W_rT$  is plotted, the infinity norm is less than -40 dB, resulting in conservative robust stability for the closed loop system.

### B. Simulation Results

Applying  $d$  as an input disturbance, the cart displacement, control effort and angle of the arm are all depicted in figure 7.

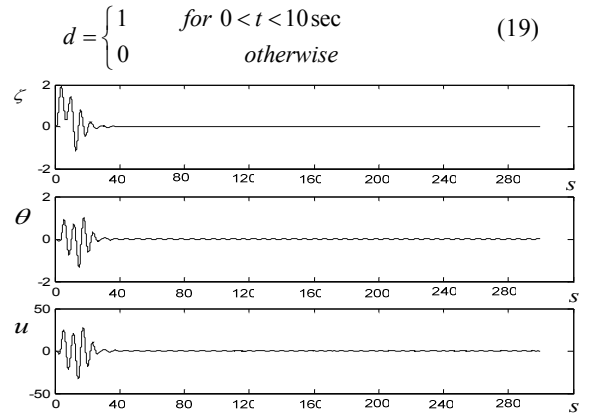


Figure 7. Simulation results of RTAC to a pulse disturbance: a) displacement, b) angle of the arm, c) control effort

Simulation results illustrate that  $\zeta$  decays just after less than 30 seconds with small amplitude fluctuations. A magnificent result is  $\theta$  has been obtained, which has settled down to zero with some small oscillations. Notice that arm does not make even a single winding and damps the input pulse disturbance with just few negligible oscillations about zero point. This implies that the control effort and consequently the control effort have been small and tolerable.

### V. MIXED $H_2/H_\infty$ CONTROLLER DESIGN

Another approach to limit the control action is to limit its energy. This can be done via an  $H_2$  optimal controller design. In order to achieve robust stability, and a desired level of performance, in presence of the control effort limitations, a simultaneous  $H_\infty$  controller design must be forwarded, while keeping the  $H_2$  norm of the control effort, at a minimum level. The multi objective problem can be formulated as following.

**Problem 2.** Design a controller  $C(s)$  in the feedback loop illustrated in figure 3, such that the following suboptimal problem is solved,

$$\left\| \begin{matrix} W_r(s)T(s) \\ W_{perf}(s)S(s) \end{matrix} \right\|_\infty \leq 1 \quad (20)$$

and simultaneously the  $\|W_u(s)U(s)\|_2$  is minimized.

The above problem can be changed into a Linear Matrix Inequality [13], and can be solved numerically using the `hinfmix` function of LMI toolbox of MATLAB. The performance of this method is also verified via simulations in this section. The LMI toolbox offers three methods to satisfy the case in problem 2. First we define:

$$N_2 = \|W_u U\|_2, \quad N_\infty = \left\| \begin{matrix} W_r T \\ W_{perf} S \end{matrix} \right\|_\infty$$

Based on this definition, the problem can be divided into three different categories by LMI approach.

#### A. Minimizing $N_2$ while $N_\infty < \gamma$

In this method we are minimizing the 2 norm of control effort so we expect almost the same results we obtained in

mixed sensitivity solution in case of the disturbance rejection. This method is advised where the control effort minimization is the main design concern and is not pursued in here.

### B. Minimizing $N_\infty$ while $N_2 < h$

In this method the control signal is allowed to become large at the very first time to reject the disturbance. In order to obtain  $h$ , the 2 norm of control effort in feasible conditions are computed.

The simulation results are shown in figure 8 where a pulse-shape disturbance with duration mentioned in (19) is rejected smoothly.

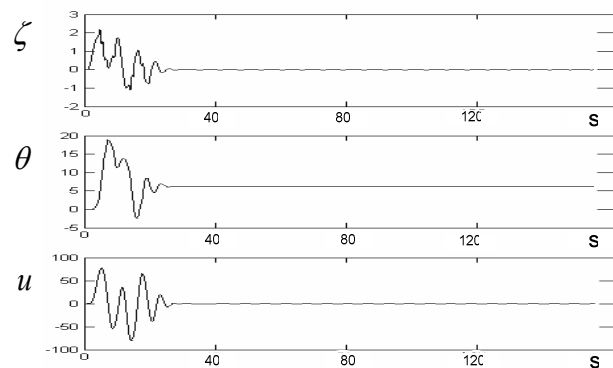


Figure 8. Simulation results of RTAC to a pulse disturbance: a) displacement, b) angle of the arm, c) control effort

Using the two norm of the control effort instead of infinity norm will improve the system performance through increasing the bandwidth from 0.6 rad/s in  $H_\infty$  design (section IV) to 1.1 rad/sec. Figure 8 shows that the arm of the RTAC rotates by one turn ( $2\pi$  rad), which it leads to a fast disturbance rejection as well as an increase in system bandwidth.

### C. Trade-off solution: $\alpha N_2 + \beta N_\infty$

The key design point in this method is choosing  $\alpha$ ,  $\beta$  such that  $H_\infty$  performance remains below 1 and control effort is limited in a feasible range. A variety of pairs could be offered for  $\alpha$  and  $\beta$  which satisfy the above criteria in  $H_2/H_\infty$  design. Among them, by Choosing  $\alpha=2$  and  $\beta=0.0005$  similar results with our previous design in part B are obtained. Where,  $H_\infty$  performance is 0.92 and the control effort is suitable for disturbance rejection.

## VI. CONCLUSIONS

In this paper a methodology to design robust controllers for the RTAC nonlinear benchmark problem for the disturbance rejection objective in presence of control effort limitation is investigated in detail. The approach employed in this paper exhibits a satisfactory disturbance rejection compared to that of other controllers reported in literature, that mainly used nonlinear or passive controllers [2,4,6] or Lyapunov methods [13]. In all of them, they are mainly dealing with sinusoidal disturbance which is generally easier to reject than pulse disturbance, taken into account in our controller design. That is we are solving a more

general problem in disturbance rejection. In addition to this, since we have taken into account the disturbance to output transfer function the presented controllers seem to provide a better robust solution to the oscillation suppression of the RTAC problem than that of [9], where a pair of desired poles has been assigned. Also comparing two main controllers designed in this paper, it is observed that in the  $H_2/H_\infty$  approach a natural way to address the control effort limitation can be used to design robust controller with larger bandwidth. In the other hand, the  $H_2/H_\infty$  simulation results proves a faster disturbance rejection –in turn of a larger control torque and consequently more windings- which is due to a less conservative criterion of controller design.

## REFERENCES

- [1] R.J. Kinsey, D.L. Mingori, and R.H. Rand, "Nonlinear controller to reduce resonance effects of a dual-spin spacecraft through precession phase lock", in Proceedings of the 31st Conference on Decision and Control, 1992, pp. 3025-30.
- [2] R.T. Bupp, D.S. Bernstein, and V.T. Coppola, "A benchmark problem for nonlinear control design: Problem statement, experimental testbed, and passive nonlinear compensation," in Proceedings of American Control Conference, 1995, pp. 4363-7.
- [3] D.K. Linder, T.P. Celano, and E.N. Ide, "Vibration suppression using a proofmass actuator operating in stroke/force saturation," Journal of Vibrations and Control, vol. 113, pp. 423-33, 1991.
- [4] R.T. Bupp, D.S. Bernstein, and V.T. Coppola, "Experimental implementation of integrator backstepping and passive nonlinear controllers on the RTAC testbed," in Proceedings of the IEEE International Conference on Control Applications, 1996, pp. 279-84.
- [5] M.Jankovic, D.Fontaine, and P.V. Kokotovic, "TORA example: cascade- and passivity-based control designs," IEEE Transactions on Control Systems Technology, 4(3) pp. 292-297, May 1996.
- [6] I.Kanellakopoulos and J.Zhao, "Tracking and disturbance rejection for the benchmark nonlinear control problem," in Proceedings of American Control Conference, 1995, pp. 4360-2.
- [7] Z.P. Jiang and I.Kanellakopoulos, "Global output-feedback tracking for a benchmark nonlinear system," IEEE Transactions on Automatic Control, 45(5), pp. 1023-7, May 2000.
- [8] C.P. Mrazek and J.R. Cloutier, "A preliminary control design for the nonlinear benchmark problem," in Proceedings of the IEEE International Conference on Control Applications, pp. 265-72, 1996.
- [9] I. Kolmanovsky, N.H. McClamroch. Hybrid feedback stabilization of rotational-translational actuator (RTAC) system, International Journal of Robust and Nonlinear Control, v 8, n 4-5, pp 367-75, April 1998.
- [10] M. Tavakoli, H. D. Taghirad, M. Abrishamchian, Identification and robust  $H_\infty$  Control of the Rotational/Translational Actuator System. Int. J. of Control Automation and System, 3(3), pp 387-396, Sep 2005.
- [11] H.D. Taghirad and P.R. Belanger, " $H_\infty$ -Based robust torque control of harmonic drive systems", Journal of Dynamic Systems, Measurements and Control, 123(3): 338-345, 2001.
- [12] G. Balas, R. Chiang, A. Packard, and M.Safanov, "Robust Control Toolbox, For use with Matlab", version 3. Mathworks, 2005.
- [13] S. Dussy, L.E. Ghaoui, "Measurement-Scheduled Control For the RTAC Problem: an LMI Approach". International Journal of Robust and Nonlinear Control, v 8, n 4-5, pp 377-400, April 1998.